J. Fluid Mech. (1975), *vol.* 68, *part* 2, *pp.* 259-271
Printed in Great Britain

Laminar plume interactions

By LUCIANO PERA
FIAT Direzione Ricerca, Turin, Italy
AND BENJAMIN GEBHART
Sibley School of Mechanical and Aerospace Engineering, Cornell University, Ithaca, New York 14853

(Received 15 August 1974)

Interactions between laminar thermal natural convection plumes generated by line and concentrated heat sources were experimentally investigated with a Mach–Zehnder interferometer. Adjacent plane plumes were found to interact more strongly than axisymmetric plumes at the same spacing. These flows with nominally free boundaries were also found to be affected by nearby surfaces which interfered with the supply of entrainment fluid. Several types of interference with plume entrainment were investigated. The nature of the interacting flows suggests a model which is successful in interpreting the mechanism. An application of the effects of plume interaction is discussed.

1. Introduction

In our earlier studies of the flow and stability of freely rising laminar thermal plumes (Lieberman & Gebhart 1969; Gebhart, Pera & Schorr 1970; Schorr & Gebhart 1970; Pera & Gebhart 1971), it was apparent that it is usually not a simple matter to achieve steady and vertical plume flows. These relatively weak flows were repeatedly seen to be affected by even very small disturbances in the laboratory. Also, the proximity of surfaces was found to have a very large influence. Presumably most such effects interact with the plume through its inevitable induced entrainment. In fact, the experimental investigation of Lieberman & Gebhart concerned the interactions of plumes in various arrays and at relatively close spacing.

Free-boundary buoyant flows are very common both in technology and in the environment. However, in many circumstances they occur multiply and their interactions and the consequences thereof are of fundamental importance. We have carried out an experimental study to determine something of the nature of such interactions. We have studied interactions between pairs of equal and unequal plane plumes and between a single plane plume and both vertical and curved surfaces. We have also studied pairs and groups of axisymmetric plumes. These observations also relate to our recent studies (Pera & Gebhart 1972, 1973) of flows generated adjacent to surfaces which have configurations leading to phenomena similar to flow separation.

Interaction characteristics were visualized and measured from interferograms

of the flow. The plane flows were generated by horizontal electrically heated wires and the axisymmetric ones by gas flames.

Most past studies of the interaction of free-boundary flows have concerned the interaction of a jet with nearby surfaces (Bourques & Newman 1960; Korbacher 1962; Sawyer 1963; Reba 1966; and others). Jets were early found to be deflected towards surfaces. With appropriate surface arrangements it was even found possible to turn a high velocity jet through an angle of 180°. Some theories and correlations have been proposed and interesting applications have arisen. The attachment of a two-dimensional jet to a neighbouring surface was found to be associated with the entrainment of surrounding fluid by the jet. Interaction between adjacent jets was studied by Miller & Comings (1960). Theoretical and experimental results were given for a dual jet.

In the recently much increased study of buoyancy-induced flows, especially of those concerned with atmospheric phenomena and those occurring in the enclosures we frequent, in processing and in bodies of water, it has become apparent that these weak flows are subject to very subtle effects. The consequences may often be very important. Man is protected in extremely cold environments because the heat released by the human body generates a natural convection layer, a thermal blanket. This remains attached to his body in spite of its irregular geometry. Attached natural convection flows also play an important role in the control of temperature and in the metabolism of plants. Circulations in enclosures heated at concentrated locations seem very complicated. In these experiments we attempted to determine something quantitative about the interactions which arise in several sufficiently well-defined and simple circumstances.

2. The experiments

In our initial investigation of the interaction between two-dimensional, or plane, thermally induced natural convection plumes, we used a horizontal array of seven parallel electrically heated nichrome wires approximately 18 cm long, 0·25 mm in diameter and spaced at 1·42 cm. Resistors in series with each wire permitted variation of the power delivered to each individual heat source from zero to a maximum level of about 73·0 W/m. This plume-array assembly was the one used by Lieberman & Gebhart (1969) for the study of heat-transfer and temperature distributions at and above an array of heated elements, for various orientations of the array.

We also report on interactions between axisymmetric plumes. Point-source plumes were generated by the heat released in burning methane gas at the exits of small vertical capillary tubes, of external diameter 1·02 mm. The amount of gas supplied was small and the diffusion flame length was never greater than about 0·5 cm. Axisymmetric plumes above heat sources of finite area were generated by burning gas above small Bunsen burners. The gas was not premixed with air. It is assumed that combustion and the gas exit velocities from the capillary tube did not have an appreciable effect, and that the resulting plume flow was similar to that which would result from a purely thermal source. This is

the method used by Yih (1952) in studying the free convection due to a point source of heat.

A 20 cm Mach–Zehnder interferometer was used to visualize the temperature fields above the heat sources. For a two-dimensional field of span 18 cm, the interferometer sensitivity was approximately 3·4 °C per fringe. No similarly simple interferometric constant applies for axisymmetric flows. The interferometer light source used was an iodine–quartz lamp provided with a green interference filter. To facilitate distance estimation, the pictures were taken with a grid of fine wires, of separation 0·51 cm, in the background.

3. The observed phenomena

The qualitative results of this study clearly indicate some very interesting interaction mechanisms between rising plumes, as well as between a single plume and adjacent surfaces. Adjacent flows and surfaces may greatly modify a buoyancy-induced flow.

Figure 1 (plate 1) shows, for reference, a single plane laminar plume in air at atmospheric pressure. Such flows are quite steady in the absence of external disturbances. However, even the single plume shows, by its slight inclination, some interaction. For air ($Pr = 0{\cdot}7$) the extent of the temperature field is approximately the same as that of the velocity field and the plume seen corresponds to essentially the whole flow field. The interference fringes are approximately isothermal contours.

Figures 2, 3 and 4 (plates 2, 3 and 4) show the interaction between two plumes of equal strength for three increasing wire lengths, about 6·4, 18 and 30·5 cm, each for five source spacings. All plumes had an equal heat input per unit span of 73·0 W/m. They were generated in a large isolated enclosure $69 \times 69 \times 84$ cm high. The five spacings used are listed in the captions along with other experimental conditions. At larger spacings and for the shorter wire lengths we see that the interaction between the plumes is weaker: that the plumes travel further before merging. This distance sharply decreases as the spacing is reduced or the wire length is increased. In all cases the merging is almost immediate at the closest spacing. We shall see that the length becomes an important parameter in the interaction, through entrainment by the plume flow. Figure 5 (plate 5) shows the interaction of a strong and a weak plume. The stronger one remains almost unaffected and the other is dominated by its presence.

For the above observations the incoming flow from below the wire array was not impeded. Figure 6 (plate 6) shows, for plumes of equal strength, the interaction when the induced flow, coming up from below, was partially restricted by an impermeable adiabatic surface located about 0·64 cm below, and parallel to, the plane of the wires. The interaction is different and merging is very much more rapid.

The effect of a nearby vertical surface on plume flow is shown in figure 7 (plate 7). The flow induced from below was not restricted. The distances between the heat source and the vertical wall were half those between the two heat sources for the plumes of equal strength in figure 3, the span of the wall being the same as

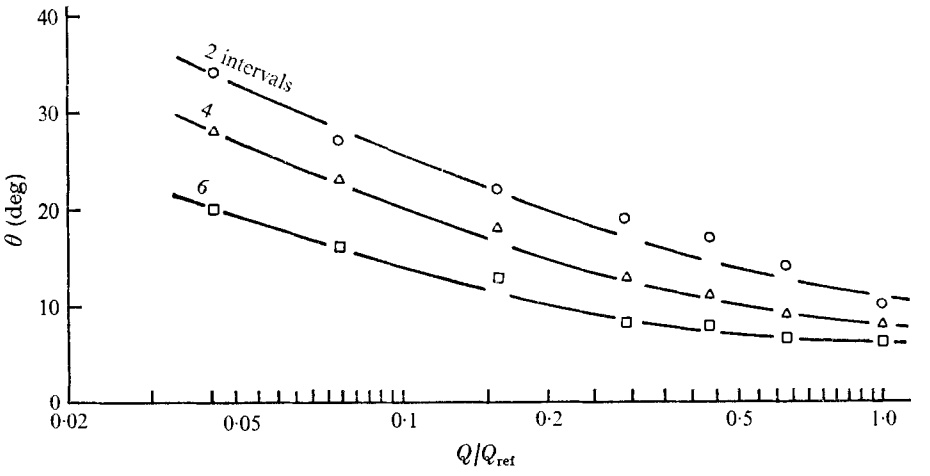

FIGURE 8. Inclination (from vertical) of a plane plume of strength Q caused by the presence of a second plume of fixed strength Q_{ref} at several spacings. Q_{ref} = 73·0 W/m. One interval = 1·42 cm.

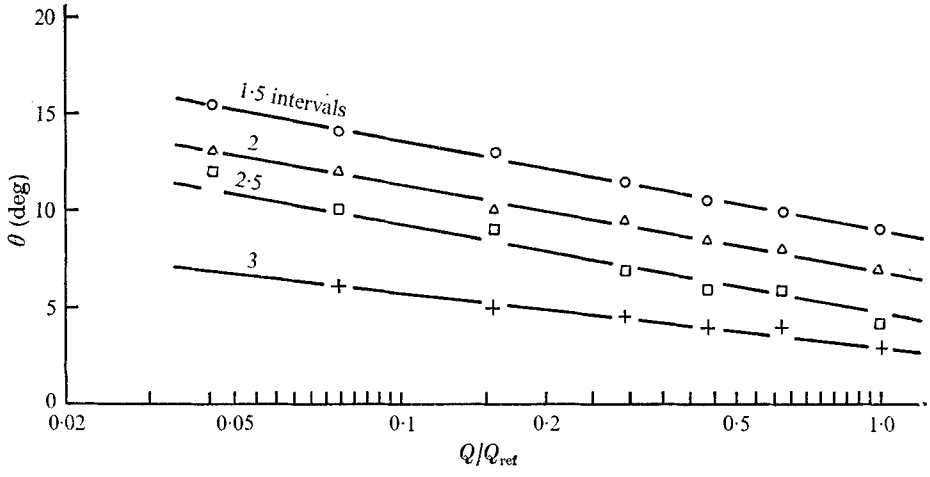

FIGURE 9. Inclination (from vertical) of a plane plume of strength Q caused by the presence of a vertical surface at several spacings. Q_{max} = 73·0 W/m. One interval = 1·42 cm.

that of the heat sources. We see, by comparison, that the effect of a wall on inclination is about the same as the effect of another plume of equal strength twice as far away. The wall restricts the entrainment flow on one side of the plume and causes the plume to be inclined towards the surface.

The characteristics of such plume interactions are seen in figures 8 and 9, where the angles of inclination from the vertical are plotted for the plume–plume and plume–wall interaction, respectively. The inclinations plotted in figure 8 are those of the smaller of two unequal plumes, for seven different smaller-plume strengths and for three different spacings. One interval is 1·42 cm. The large plume was at a fixed strength of 73·0 W/m throughout. In figure 9 the inclination change with increasing power is shown for different spacings from a vertical

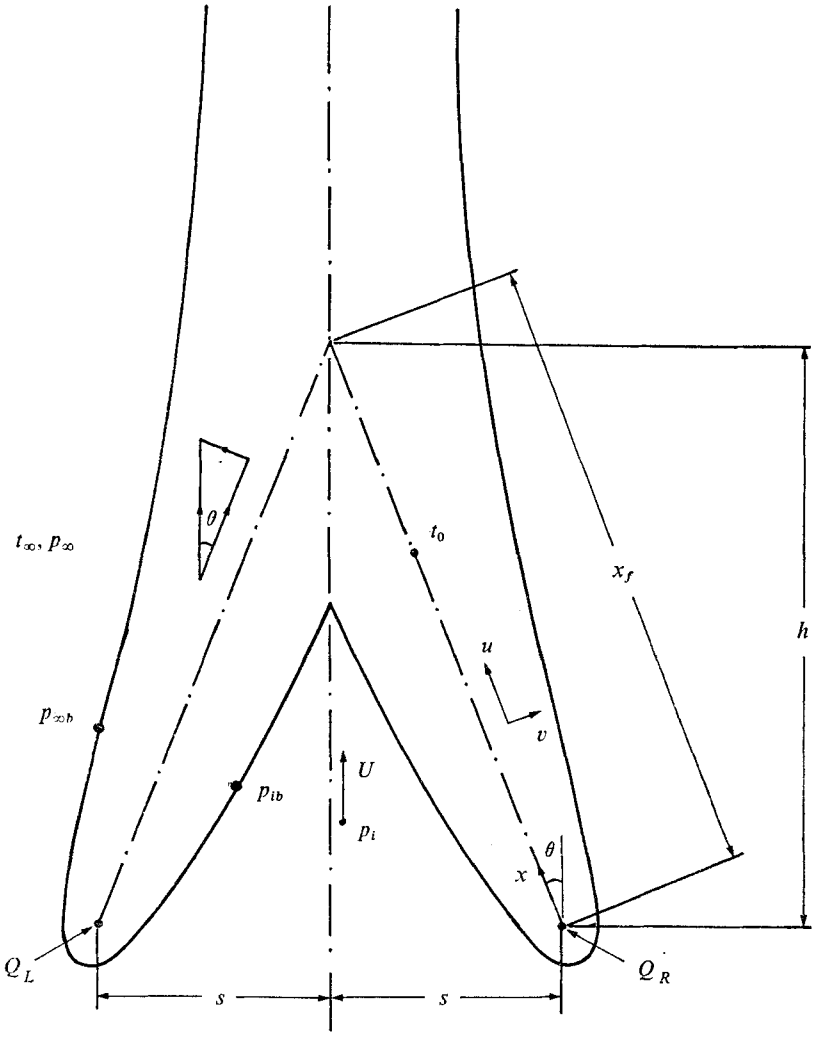

FIGURE 11. Plane-plume interaction.

surface. The angle of inclination is seen to be much greater at lower spacings for both configurations and especially so when a weak plume interacts with a stronger one. We shall present our extensive data on unequal plumes in detail in a later publication.

Figure 10 (plate 8) shows interferograms of the flow in the presence of an adjacent half-cylindrical surface, at several spacings. The plume is seen to approach, become attached to and turn with the surface, even following it to the top at close spacing. This behaviour may be compared with the bending of a jet by an adjacent surface. However, in buoyancy-induced flows the turning while attached is apparently limited by buoyancy to about 90°.

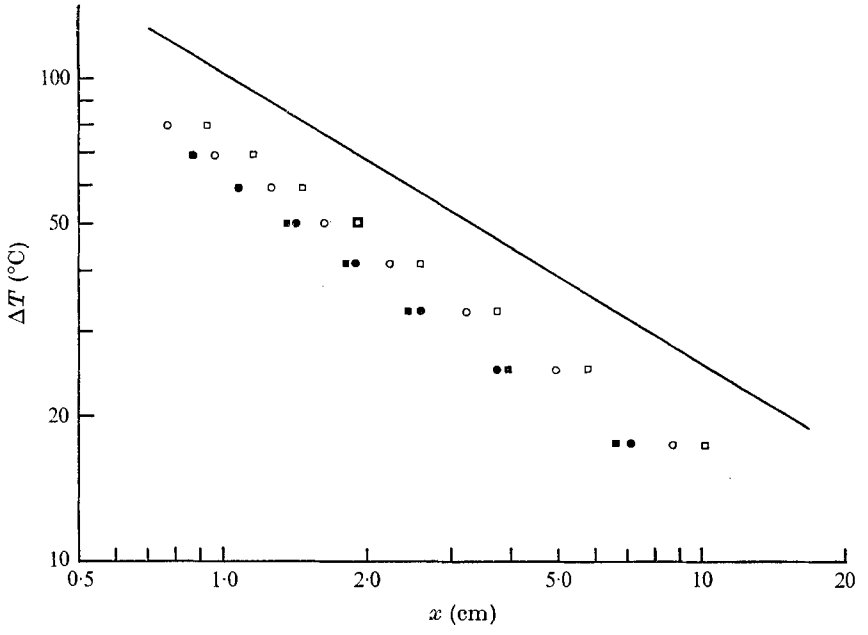

FIGURE 12. Measured mid-plane temperature decay for the interacting plane plumes in figures 3(*b*) and (*c*). (*b*) □, left plume; ○, right plume. (*c*) ■, left plume; ●, right plume.

4. Entrainment prediction of interaction

The experimental results for the interaction of relatively free plumes, of constricted ones and of a plume near an impermeable wall all suggest that the basic mechanism is the limitation or restriction of the flow which supplies the fluid entrained downstream by the plume. This is the natural convection equivalent of a Coanda effect. The demands of entrainment cause a flow inducing pressure inhomogeneity in the external fluid, especially on the constricted side. However, close similarity ends there. In forced flow, the jet momentum is the agency which induces this pressure field. In buoyancy-induced flows it is, apparently, the component of the buoyancy force normal to the principal flow direction that causes the pressure difference which drives the flow of the external fluid which will eventually be entrained.

We here develop a theory for the idealized interaction shown in figure 11. An inviscid expression relates the induced flow of velocity U in the region between the plumes to the difference between the dynamic pressure p_i there, and the dynamic pressure p_∞ in the ambient external medium. The difference $p_\infty - p_i$ arises from the cross-plume component of the buoyancy force. Then, through continuity considerations, we relate U to the entrainment rate $v(\infty)$ required by each plume on the side of the interaction, in the region $0 \leqslant x \leqslant x_f$.

The use of a boundary-layer similarity formulation for these inclined plumes initially appears justified from several separate considerations. First, we can see in figures 2–4 that the inclined plumes, especially those at the larger spacings,

have essentially straight centre-lines. They are nearly plane plumes. Second, the measured downstream decay of the midplume temperature $t_0 - t_\infty$ was found to be approximately as $x^{-\frac{3}{5}}$. This is the decay predicted by analysis for vertical plane plumes and corroborated through measurements, e.g. by Schorr & Gebhart (1970). However, measured temperature levels are always appreciably lower than those calculated. The collection of our present data given in figure 12 shows about the same decay and is similarly below the theory.

Therefore, we treat these inclined flows as vertical ones, with the buoyancy force $g\rho\beta(t-t_\infty)$ in the Grashof number Gr_x reduced by a factor $\cos\theta$. The following similarity transformation is well known (see Gebhart *et al.* 1970) as specialized to a plane plume. The co-ordinates, velocities, etc., are defined in figure 11.

$$u = \psi_y, \quad v = -\psi_y, \quad \psi = \nu c(x) f(\eta), \quad \phi(\eta) = (t-t_\infty)/(t_0-t_\infty), \quad \eta = b(x)y,$$

where $$c(x) = G, \quad b(x) = \frac{G}{4x}, \quad G = 4\left(\frac{Gr_x}{4}\right)^{\frac{1}{4}}, \quad Gr_x = \frac{g\beta x^3(t_0-t_\infty)\cos\theta}{\nu^2},$$

$$t_0 - t_\infty = N x^{-\frac{3}{5}},$$

$$N = \frac{1}{4}\left[\frac{Q^4}{\rho^4 c_p^4 \nu^2 g\beta I^4 \cos\theta}\right]^{\frac{1}{5}}, \quad I = \int_0^\infty f'\phi\, d\eta.$$

The solutions, in terms of the stream and temperature functions f and ϕ, are known for many values of the Prandtl number Pr.

The local (at x) dynamic pressure difference immediately across the boundary region of a plume is denoted as $p_{\infty b} - p_{ib}$. This difference is taken to be the result of, or the balance for, the cross-plume buoyancy component $g\rho\beta(t-t_\infty)\sin\theta$ integrated across the boundary region. With boundary-layer approximations, this becomes, in terms of usual quantities,

$$\Delta p_b = p_{\infty b}(x) - p_{ib}(x) = 2\int_0^\infty \rho g\beta(t-t_\infty)\sin\theta\, dy$$

$$= \frac{\rho\nu^2}{8x^2} G^3 \tan\theta \int_0^\infty \phi\, d\eta \propto x^{-\frac{1}{5}}.$$

This difference Δp_b differs from $p_\infty - p_i = \Delta p$, defined above, by an amount of the order of the dynamic pressure characteristic of the normal velocity component $v(\infty)$ of the fluid drawn in by the plume flow for entrainment. Now the normal component of velocity is given by $-v(\infty) = (3\nu/5x)\, Gf(\infty) \propto x^{-\frac{2}{5}}$. The equivalent dynamic pressure, divided by Δp_b, for comparison, becomes

$$\frac{\rho[v(\infty)]^2}{2\Delta p_b} = 36 f^2(\infty) \Big/ 25 G \tan\theta \int_0^\infty \phi\, d\eta.$$

This is of order $1/G$ and may be neglected, to our approximation, and Δp_b may be taken as Δp. (Note that the $v(\infty)$ effects on opposite sides are opposite and would tend to cancel.)

Another question is whether the presence of $\Delta p \propto G^3/x^2$, and the x variation it may have, will have an important effect on the plume flow. The characteristic

buoyancy-induced velocity U_c is seen from the formulation to be proportional to G^2/x. The dynamic pressure associated with it, which is of first order, is G^4/x^2. The ratio of Δp to this is again $1/G$ and, therefore, negligible. Thus, we formulate the plume flow as that of a plane plume in an inviscid region of zero dynamic pressure, but with a reduced buoyancy force.

Now, considering the inviscid induction of fluid up from below and into the region between the plumes, we may write down the Bernoulli equation. We shall assume that both p_i and U are uniform across the space between the plumes at any given height, i.e. $p_i(x)$ and $U(x)$. The result is

$$p_\infty - p_i = \frac{\rho U^2}{2} = \frac{\rho \nu^2}{8x^2} G^3 \tan\theta \int_0^\infty \phi \, d\eta \propto x^{-\frac{1}{5}}. \tag{1}$$

Recall that $\Delta p = \Delta p_b$.

We have the surprising result, since $G \propto x^{\frac{3}{5}}$, that $U \propto x^{-\frac{1}{10}}$. Given this very weak variation, we shall approximate U throughout the region between the plumes by its average value calculated over $0 \leqslant x \leqslant x_f$ using (1):

$$\overline{U} = \frac{1}{x_f}\int_0^{x_f} U(x)\,dx = \tfrac{10}{9} U_{x_f} = \tfrac{10}{9} U_f = \frac{10\nu G_f}{18 x_f}\left(G_f \tan\theta \int_0^\infty \phi \, d\eta\right)^{\frac{1}{2}}, \tag{2}$$

where $G_f = G_{x_f}$.

This estimate applies over the area across which the fluid to be entrained enters the region between the plumes. This area is estimated as $A = 2sL + 2hs$, where L is the equal span of the two plumes, s is half their spacing and h is defined in figure 11. We note here that this is a systematic over-estimation of A because it ignores the plume thickness. The flow rate $\overline{U}A$ supplies the combined entrainment LV by the two plumes on their inside faces, which is calculated from $v(\infty)$ as

$$LV = 2L \int_0^{x_f} -v(\infty)\,dx = 2\nu L G_f f(\infty) \tag{3}$$

and

$$A\overline{U} = 2s(L+h)\,\overline{U} = LV = 2\nu L G_f f(\infty). \tag{4}$$

Noting that $\tan\theta = s/h$ and that $x_f^2 = s^2 + h^2$ the above relation between G_f and h/s becomes

$$\left[10\left(\int_0^\infty \phi \, d\eta\right)^{\frac{1}{2}} \Big/ 18 f(\infty)\right] G_f^{\frac{1}{2}} \left(1 + \frac{h}{L}\right) = \left[\frac{h}{s}\left(\frac{h^2}{s^2} + 1\right)\right]^{\frac{1}{2}}.$$

This may be written in terms of a more convenient Grashof number based on Q and s defined as follows:

$$Gr_Q^{\frac{1}{5}} = (g\beta s^3 Q/k\nu^2)^{\frac{1}{5}} = G_Q,$$

for which

$$G_f = 2G_Q \left(\frac{1}{Pr\, I}\right)^{\frac{1}{5}} \left(\frac{h^2}{s^2} + 1\right)^{\frac{1}{6}} \left(\frac{h}{s}\right)^{\frac{1}{5}},$$

where

$$I = \int_0^\infty \phi f' \, d\eta$$

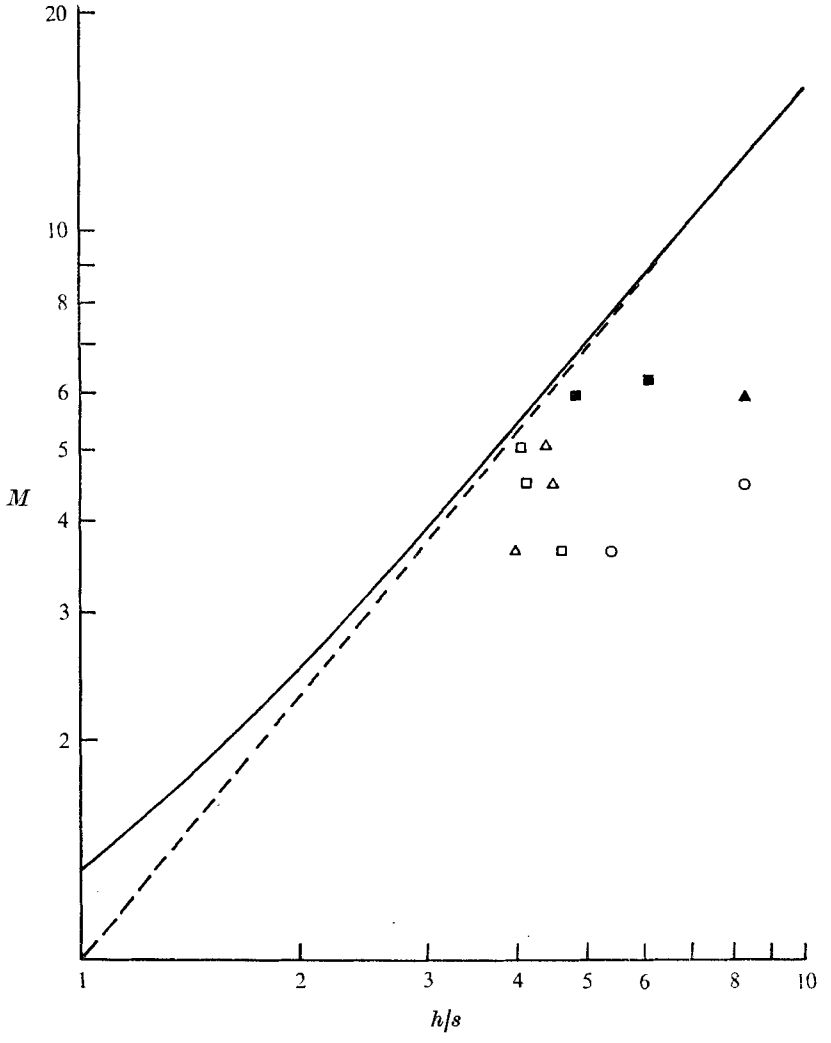

FIGURE 13. Comparison of theory and data, without the end-flow area effect $1+h/L$. ○, data from figure 2; △, data from figure 3; □, data from figure 4; ▲, data obtained by extrapolation from upper interferograms of figure 3; ■, similar data from figure 4.

is a non-dimensional measure of the rate of energy convection in the plume. The relation between G_Q and h/s becomes

$$\left[\frac{10\sqrt{2}}{18f(\infty)}\left(\int_0^\infty \phi\, d\eta\right)^{\frac{1}{2}}\left(\frac{1}{PrI}\right)^{\frac{1}{10}}\right]\left(1+\frac{h}{L}\right)G_Q^{\frac{1}{2}} = P\left(1+\frac{h}{L}\right)G_Q^{\frac{1}{2}} = M = \left[\frac{h}{s}\left(\frac{h^2}{s^2}+1\right)\right]^{\frac{2}{5}}. \tag{5}$$

The value of P is found from the results of Gebhart *et al.* (1970) to be 1·11 for air ($Pr = 0{\cdot}7$).

The above relation for plumes of infinite span, i.e. $h/L = 0$, is plotted in figure 13 as M *vs.* h/s. The result is the solid curve. The dashed curve is the approximation resulting from neglecting 1·0 compared with h^2/s^2. Points determined from the

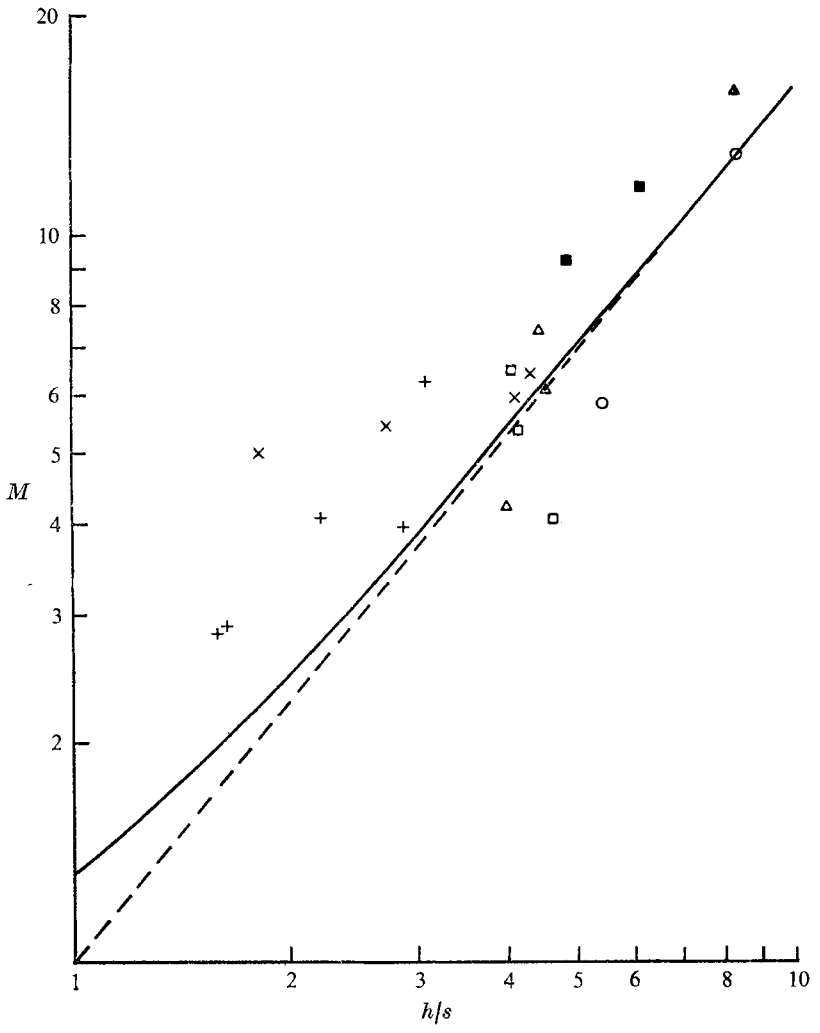

FIGURE 14. Comparison including the end-flow area, for the data of figures 2–4. +, data for equal but restricted plumes from figure 6; ×, data for plume–wall interaction from figure 7. Other symbols as in figure 13.

data on figures 2–4 are seen to lie at values of h larger than those predicted by the theory. The data are also scattered in terms of h/L, the disagreement being greater for plumes of smaller span L. These disagreements clearly suggest the importance of end flows. Retaining that term, i.e. $1+h/L$, in M, the theory and data are replotted in figure 14. This makes all the data at larger s closely follow a single trend, which parallels the theory. The experimental values of h/s are, remarkably, only about 25 % below the theory. The results at very close spacing still lie above the theory. The interferograms suggest that these latter flows are far from a boundary-layer state.

We might also expect that the plume–surface interaction shown in figure 7 is similar to the interaction of equal plumes, except for the no-slip condition at the

surface. Data from figure 7 are also shown on figure 14. Interaction at larger values of s is seen to be quite similar to that between plumes and the agreement with the theory is again seen to be good.

The interactions shown in figure 6, with an impermeable plane positioned a distance d below and parallel to the plane in which the plume sources lie, require a change in the flow area related to $\overline{U}$. The value $2s(L+h)$ was used before. Now the proper estimate is $d(4s+2L)+2hs$. The resulting relation between G_Q and h/s becomes

$$P\left(\frac{2d}{L}+\frac{d}{s}+\frac{h}{L}\right)G_Q^{\frac{1}{2}} = M = \left[\frac{h}{s}\left(\frac{h^2}{s^2}+1\right)\right]^{\frac{2}{3}}.$$

The data for the interactions of figure 6 are also plotted in figure 14 as M *vs.* h/s. Again the data follow the same trend at larger s.

Our model is seen to be quite successful in bringing together all the data for flows at larger spacing. These appear to be more accurately of boundary-layer form. Thus, an entrainment limitation seems confirmed as the mechanism which controls plume interaction. The systematic 25% difference is thought to be related to approximations in our analysis. In particular, the over-estimate in A would cause a difference in this direction. However, we have not made any quantitative calculations of this effect.

5. Axisymmetric plumes

Interferograms of the interaction of such plumes, generated by the combustion of methane in diffusion flames, over both point and disk heat sources are reproduced in figures 15 and 16 (plates 9 and 10) respectively. The fringe patterns do not represent, as they do in two-dimensional flows, the actual temperature field or flow extent. Since the interferometer light beam crosses regions of varying depth and of non-uniform temperature, over the field, a point-by-point fringe-shift integration is needed to determine corresponding temperature distributions. In addition, the gradients in chemical composition also cause index-of-refraction gradients.

We see in figures 15 and 16 that the interaction of adjacent axisymmetric flows is much less profound than that found between plane flows, at the same spacing. This indicates that the presence of a flow restriction near an axisymmetric plume does not so severely restrict its entrainment mechanism. However, as for plane plumes, shortly after the plumes come in contact, the individual plumes are no longer distinguishable. Their combination will eventually become a single plume rising as if from a single source.

Lieberman & Gebhart (1969), in studying heat transfer in an array of parallel heated wires, having the same energy input, found that the wires at the centre were cooler than those at the edges of the array. The analogy of this effect is apparent in our results and is very interesting. Adjacent plane plumes and walls suppress the lateral component of the flow of fluid for entrainment. Thus, a larger flow will be induced from the region below. The forced-flow aspect of this incoming flow is the cause of the increased heat-transfer coefficients found by Lieberman &

Gebhart for the wires in the centre of their array. An identical effect occurs with multiple point-source plumes. This is seen in the flame separation from the middle nozzle of the seven-plume array of figure 15. Higher heating rates in this configuration actually caused the flames from the central burners to blow out.

6. Conclusions

The foregoing observations clarify certain aspects of the interaction of multiple free-boundary buoyancy-induced flows. The postulate of the decisive influence of the entrainment mechanism is very well supported by the success of the approximate theory with different arrangements.

Flow interaction between plumes has direct technological applications, e.g. in the design of an array of cooling towers. At present, when structural considerations limit the size and capacity of the towers, several of them may be needed for a single plant. They are usually widely spaced, apparently to eliminate any interaction. Flat areas are preferred to avoid any effects of adjacent slopes. Our experimental results suggest instead that a spacing which would enhance plume interaction might be more desirable. Interaction will generate a much stronger single plume, which will be able to rise higher in the atmosphere than the individual weaker plumes. The combined plume may be more resistant to side winds. It would perhaps sometimes penetrate an inversion layer. One might surmise that, if several towers were close together in a polygonal array, not only would a single strong plume form, but also the low pressure region formed in the inner core would offer interesting possibilities. This might be an optimum location for additional units at higher working efficiencies. Of course, a particular array might be optimized through appropriate combinations of wet, dry and forced towers.

The authors wish to acknowledge support from the National Science Foundation under Research Grant GK-18529 for this research, as well as the help of Mr Hussain Shaukatullah in interpreting the interferograms.

REFERENCES

BOURQUES, C. & NEWMAN, B. G. 1960 Reattachment of a two-dimensional incompressible jet to an adjacent flat plate. *Aero. Quart.* **11**, 201–232.

GEBHART, B., PERA, L. & SCHORR, A. W. 1970 Steady laminar natural convection plumes above a horizontal line heat source. *Int. J. Heat Mass Transfer*, **13**, 161–171.

KORBACHER, G. K. 1962 The Coanda effect at deflection surfaces detached from the jet nozzle. *Can. Aero. Space J.* **8**, 1–6.

LIEBERMAN, J. & GEBHART, B. 1969 Interactions in natural convection from an array of heated elements, experimental. *Int. J. Heat Mass Transfer*, **12**, 1385–1396.

MILLER, D. R. & COMINGS, E. W. 1960 Force-momentum fields in a dual-jet flow. *J. Fluid Mech.* **7**, 237–256.

PERA, L. & GEBHART, B. 1971 On the stability of laminar plumes: some numerical solutions and experiments. *Int. J. Heat Mass Transfer*, **14**, 975–984.

PERA, L. & GEBHART, B. 1972 Experimental observations of wake formation over cylindrical surface in natural convection flow. *Int. J. Heat Mass Transfer*, **15**, 175–177.

PERA, L. & GEBHART, B. 1973 On the stability of natural convection boundary layer flow over horizontal and slightly inclined surfaces. *Int. J. Heat Mass Transfer*, **16**, 1147–1163.

REBA, I. 1966 Applications of the Coanda effect. *Sci. Am.* **214**, 84–92.

SAWYER, R. A. 1963 Two-dimensional reattaching jet flows including the effects of curvature on entrainment. *J. Fluid Mech.* **17**, 481–498.

SCHORR, A. W. & GEBHART, B. 1970 An experimental investigation of natural convection wakes above a line heat source. *Int. J. Heat Mass Transfer*, **13**, 557–571.

YIH, C. S. 1952 Free convection due to a point source of heat. *Proc. 1st U.S. Nat. Cong. Appl. Mech.*, pp. 941–947.

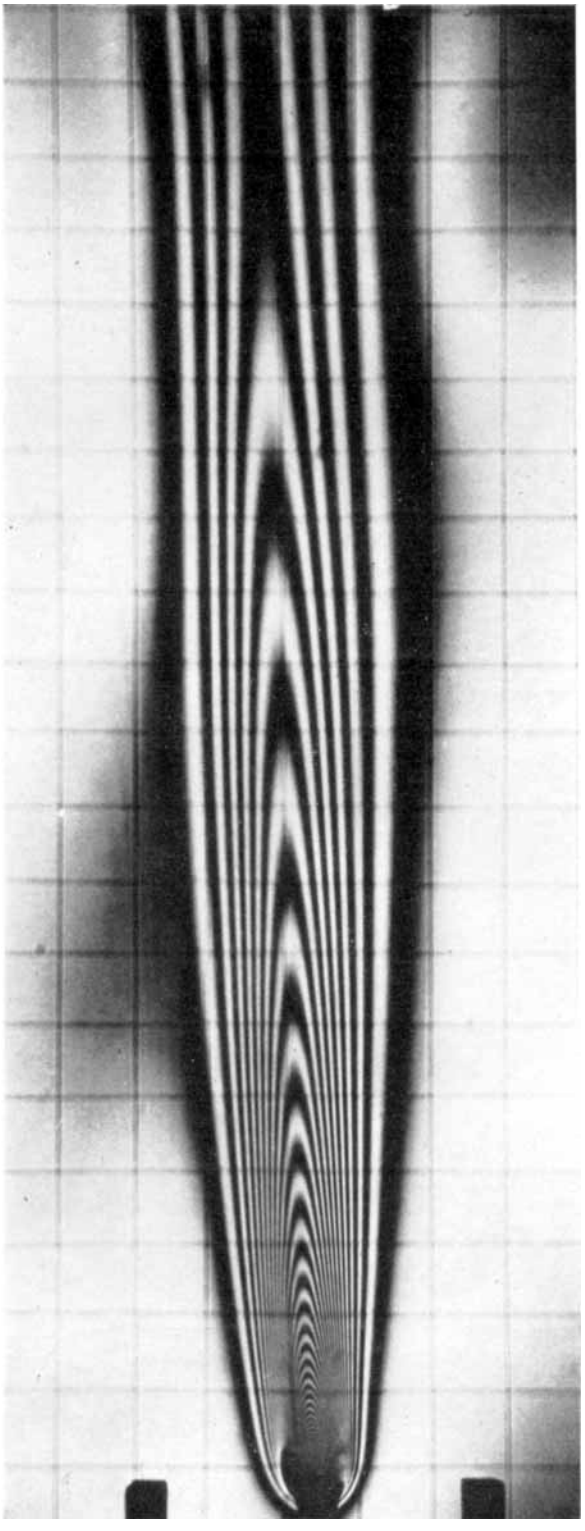

FIGURE 1. Single plane plume in air at atmospheric pressure. Wire length = 18 cm, wire diameter = 0·25 mm, heat dissipated in the wire = 73·0 W/m, approximate interferometric constant = 0·61 °C/fringe m, distance between grid lines = 0·63 cm.

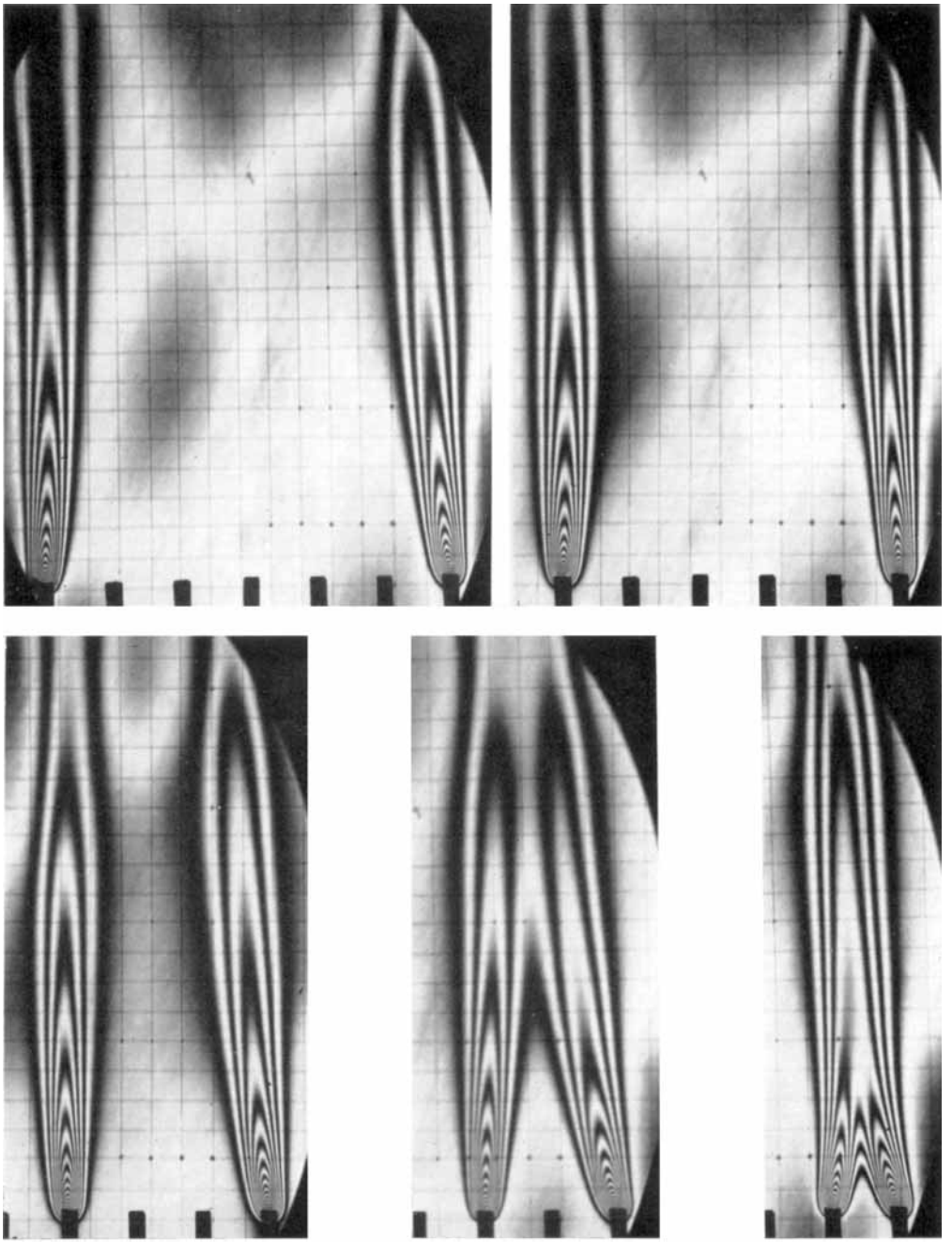

FIGURE 2. Flow interaction between plane plumes of equal strength. Wire length = 6·4 cm, other conditions as in figure 1. Distances between sources are 8·48, 7·16, 4·29, 2·87 and 1·42 cm respectively.

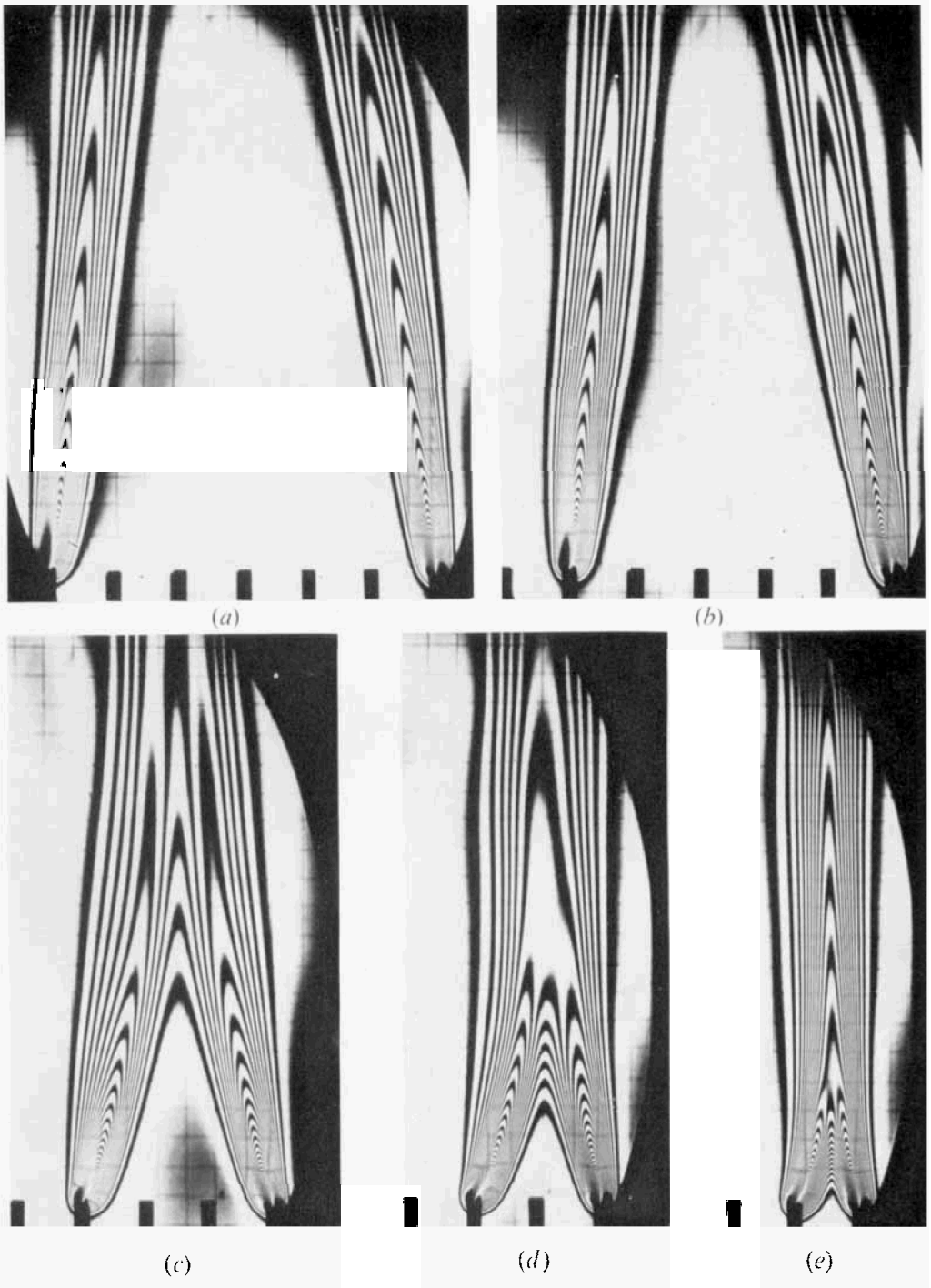

FIGURE 3. Wire length = 18 cm, other conditions as in figure 2.

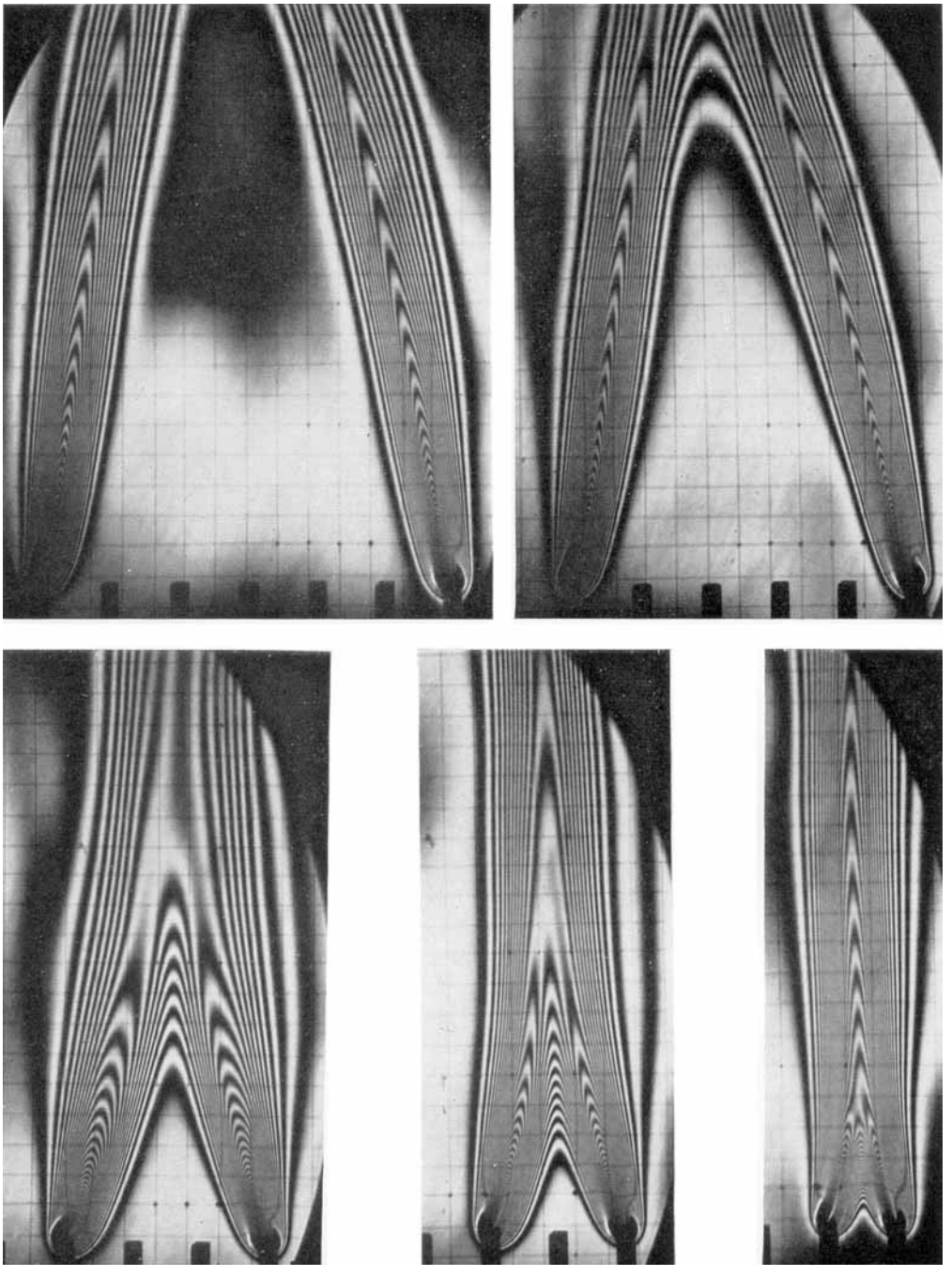

FIGURE 4. Wire length = 30·5 cm, other conditions as in figure 2.

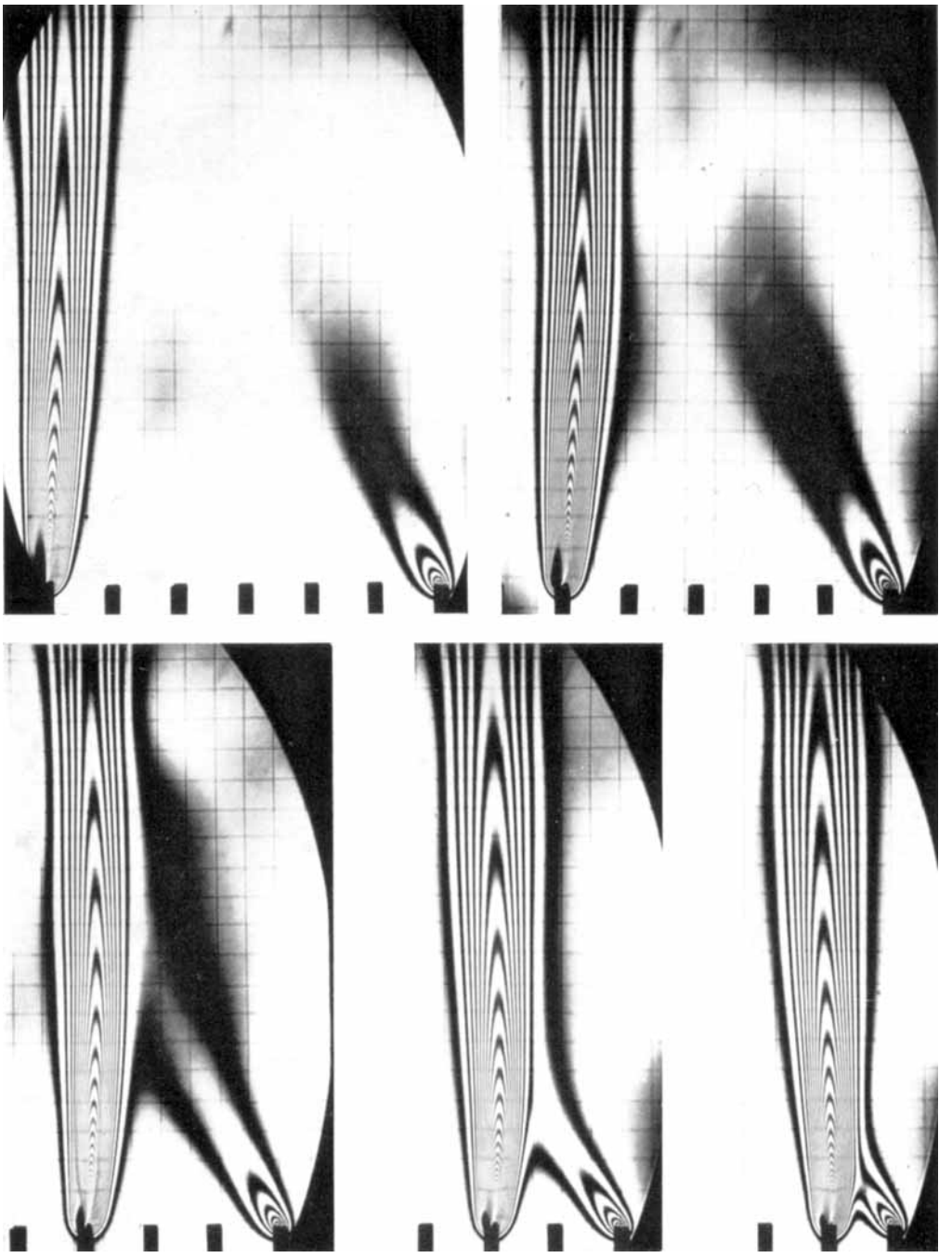

FIGURE 5. Flow interaction between plane plumes of unequal strength. Distance between sources as in figure 2, other conditions as in figure 1. Heat dissipated in wires is 73·0 and 2·95 W/m respectively.

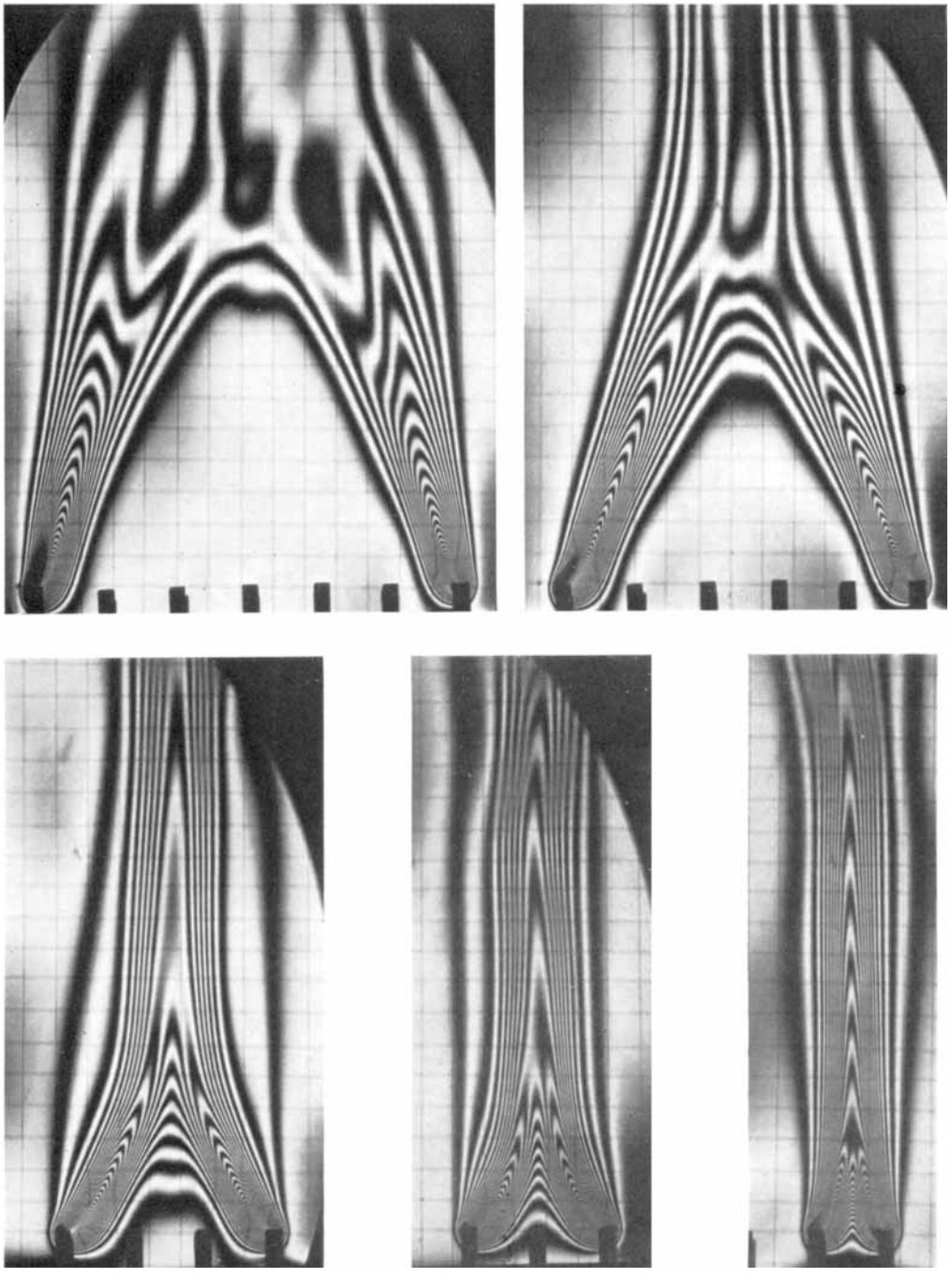

FIGURE 6. Flow interaction between plane plumes of equal strength when incoming flow from the bottom is partially restricted. Other conditions as in figures 1 and 2.

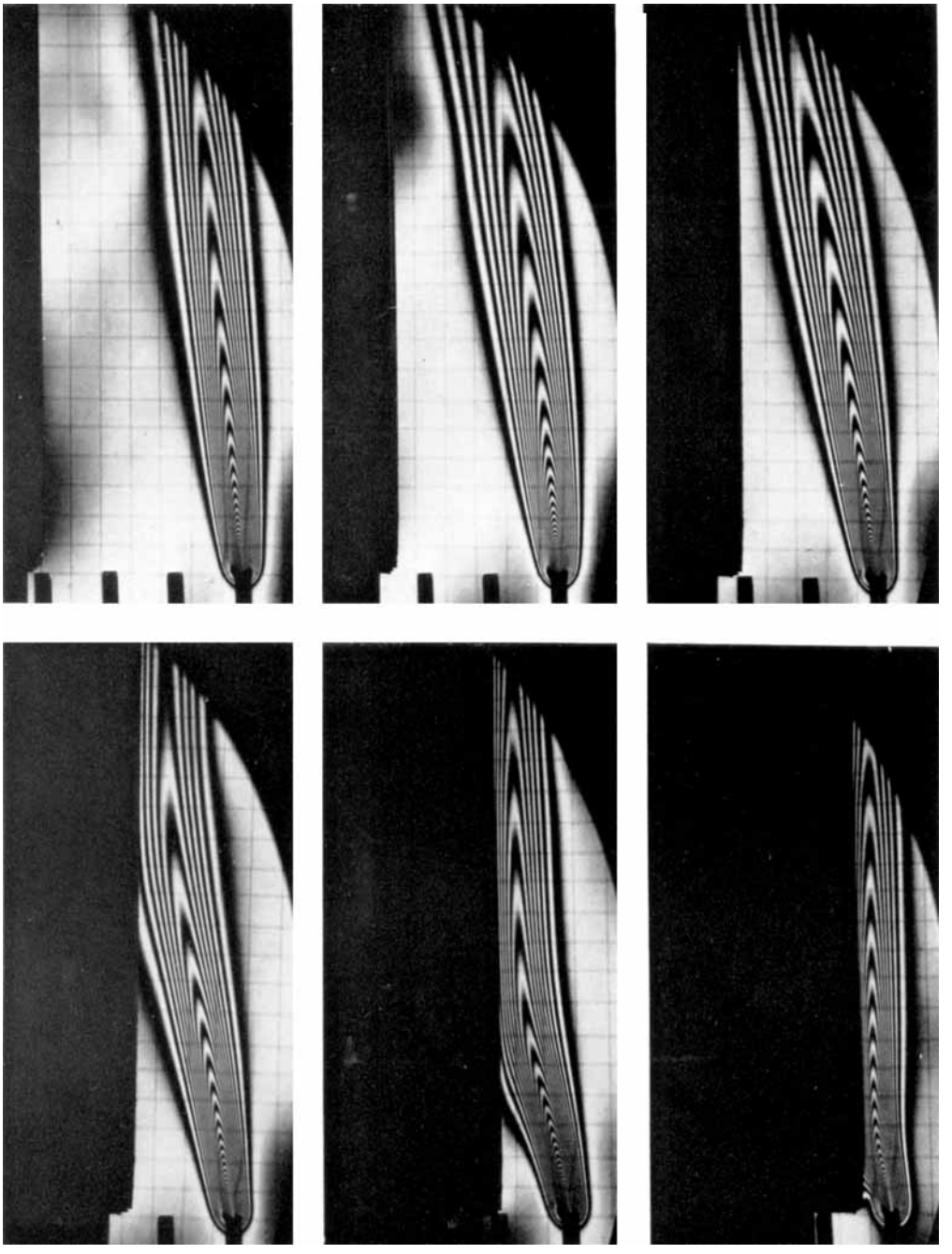

FIGURE 7. Effect of an adjacent vertical surface on plane-plume flow. Distances between wall and heat sources are 0·71, 1·42, 1·91, 2·62, 3·30 and 4·03 cm respectively, other conditions as in figure 1.

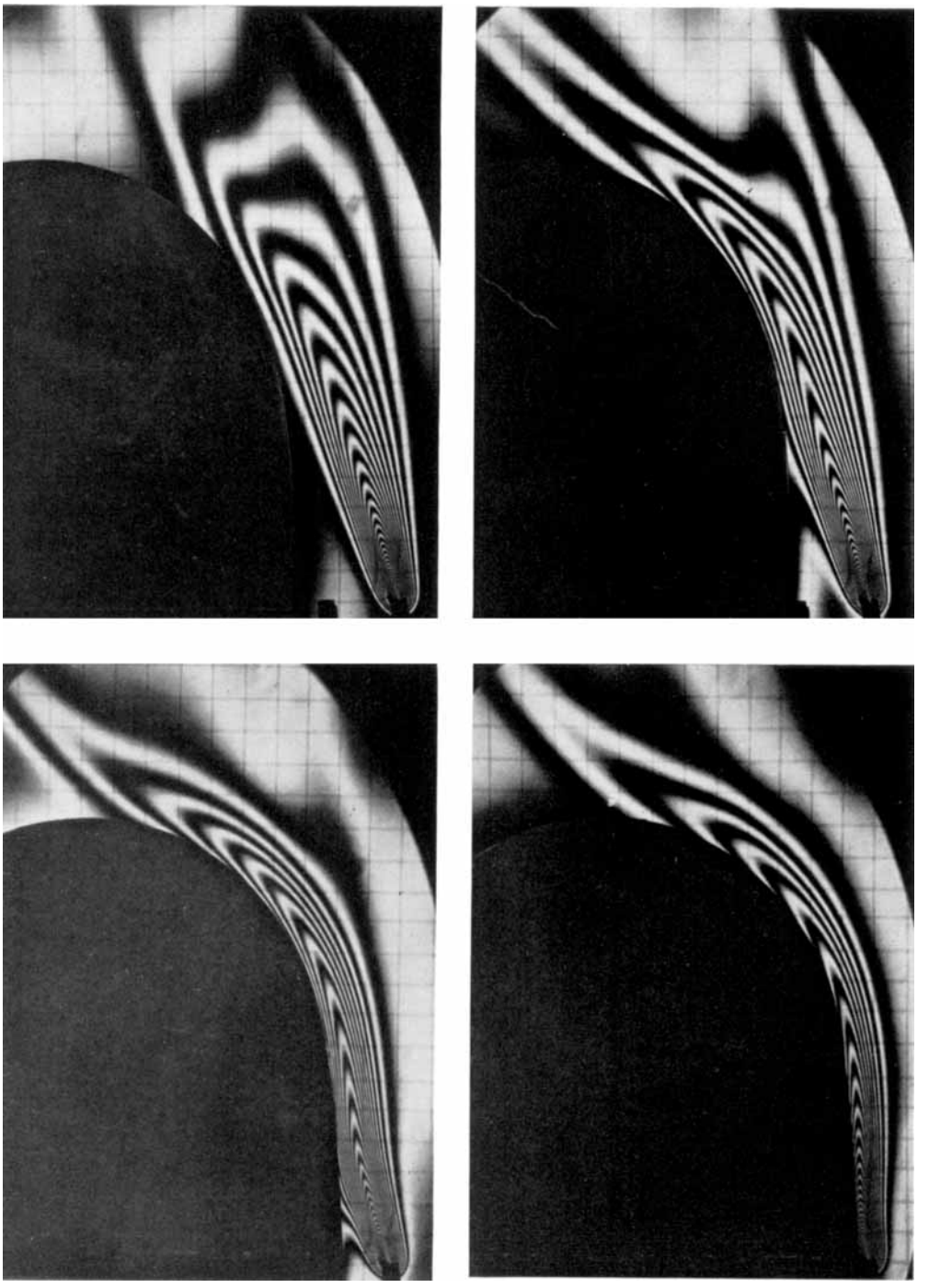

FIGURE 10. Effect of an adjacent semi-cylindrical surface on plane-plume flow. Diameter of cylindrical surface = 9·5 cm, other conditions as in figure 1.

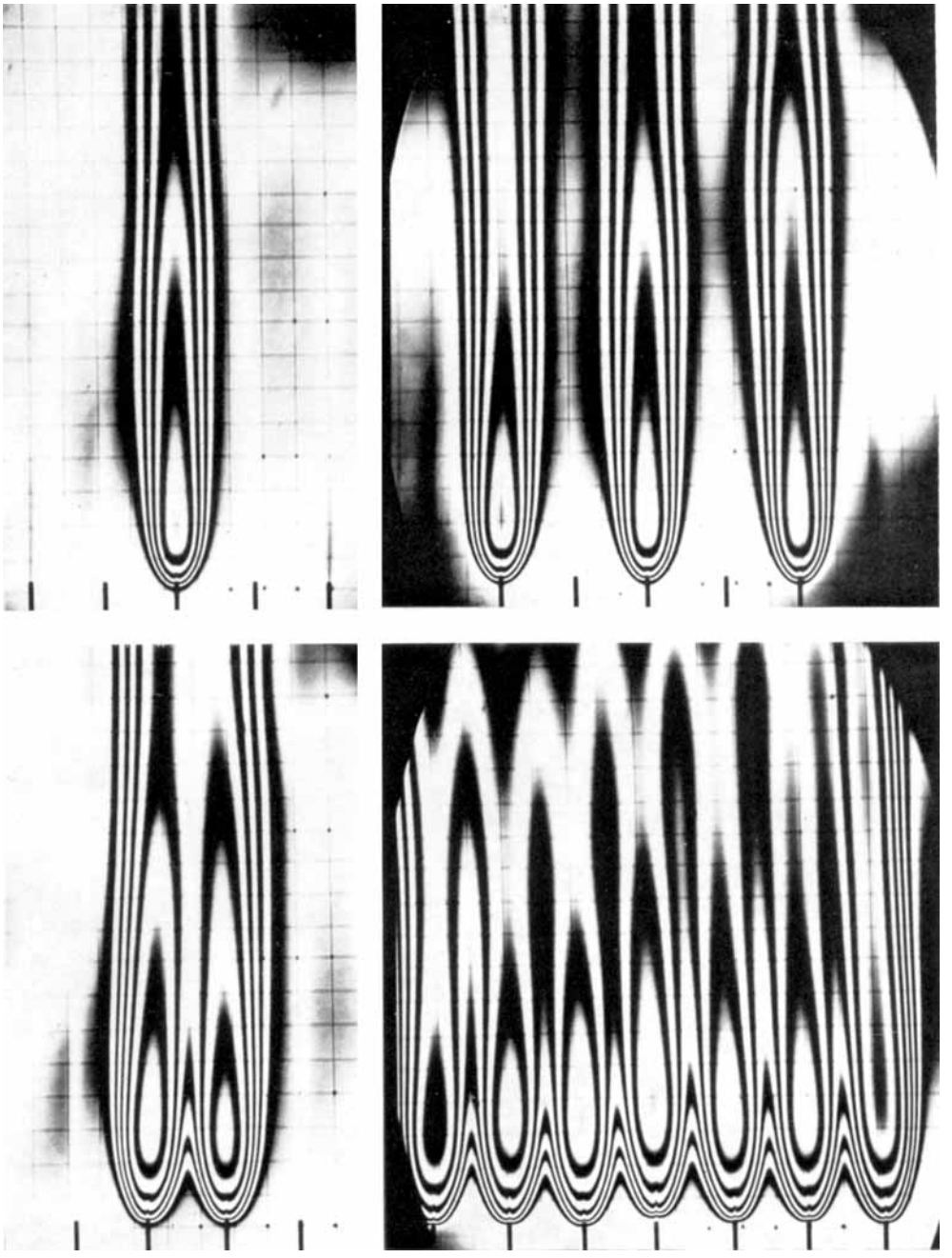

FIGURE 15. Single and combined axisymmetric plumes over point heat source in air at atmospheric pressure. Distances between sources are 2·84 and 1·42 cm, diameter of sources = 0·51 mm.

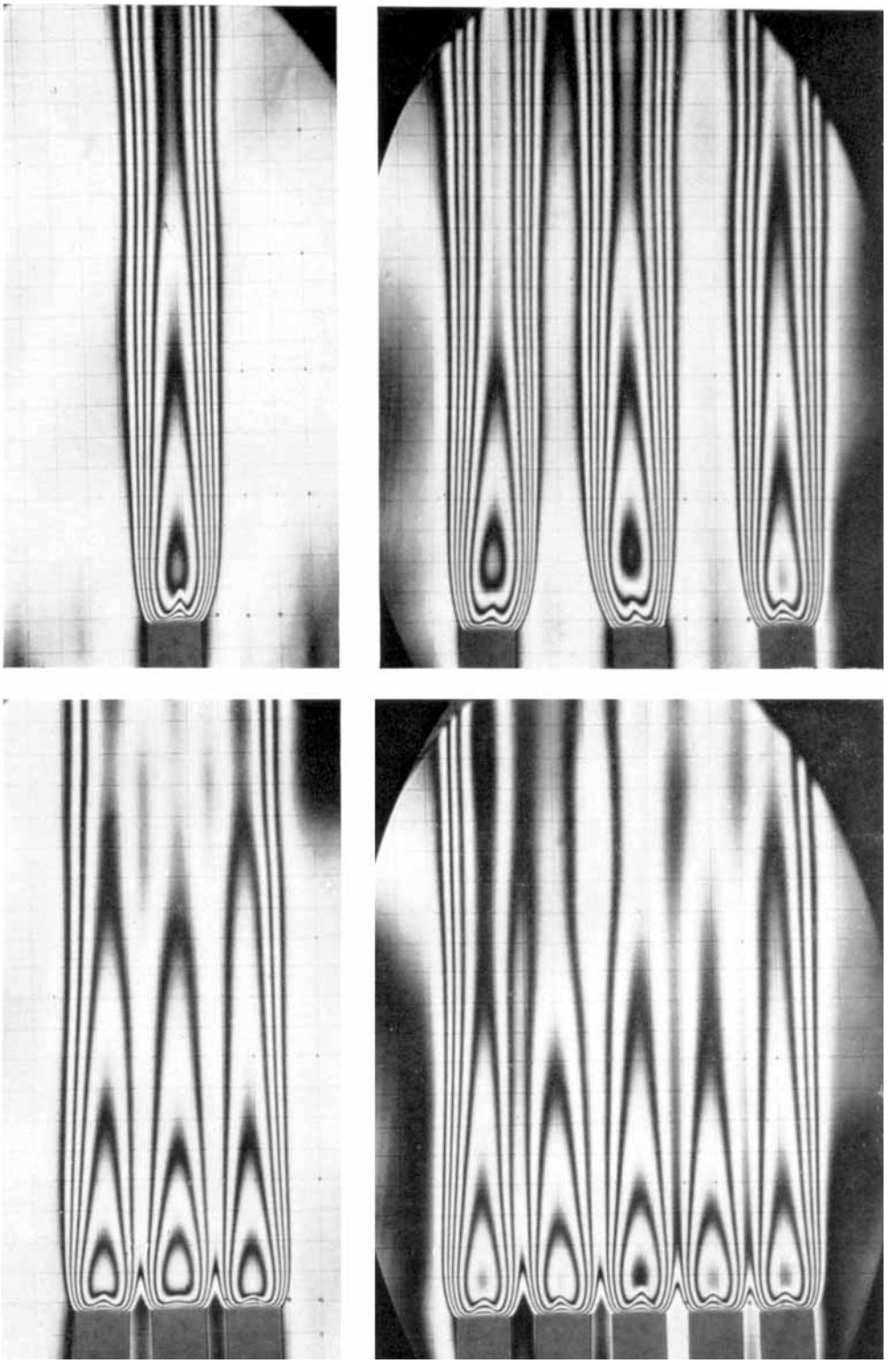

FIGURE 16. Single and combined axisymmetric plumes over heat sources of finite area in air at atmospheric pressure. Distances between sources are 2·84 and 1·42 cm, diameter of sources = 1·1 cm.